Surface phonon modes of the RbBr(001) crystal surface by inelastic He-atom scattering

G. Chern and J. G. Skofronick
Department of Physics, Florida State University, Tallahassee, Florida 32306-3016
and Center for Materials Research and Technology (MARTECH), Florida State University, Tallahassee, Florida 32306-3016

W. P. Brug and S. A. Safron
Department of Chemistry, Florida State University, Tallahassee, Florida 32306-3006
and Center for Materials Research and Technology (MARTECH), Florida State University, Tallahassee, Florida 32306-3016
(Received 27 December 1988)

Inelastic He-atom scattering ($k_i \approx 7$ Å^{-1}) was used to measure the dynamics of the RbBr(001) crystal surface ($T_s \approx 115$ K). Time-of-flight spectra taken in two high-symmetry directions, ⟨100⟩ and ⟨110⟩, were analyzed to give the surface dispersion curves for the entire surface Brillouin zones $\bar{\Gamma}\bar{X}$ and $\bar{\Gamma}\bar{M}$. The Rayleigh mode and its geometric "folded," optical surface resonance (expected from the quasimonatomic behavior due to the nearly equal masses of the Rb^+ and Br^- ions) were observed; the data also suggest the existence of another optical surface feature in the optical band. Although calculations had suggested that this crystal should have important surface relaxation effects, the main one being a surface-localized optical branch lying above the optical band, no evidence of this was seen. Moreover, the calculated surface dispersion curves for the unrelaxed surface appear to fit the measurements slightly better than those for the relaxed surface, although neither predicts the optical resonance mentioned above. Finally, these observed differences provide guidance on the use of the shell model for describing the physics of ionic insulator crystals.

I. INTRODUCTION

The RbBr(001) surface is interesting for several reasons. (1) Slab-dynamics calculations of its surface dynamics have been carried out, which predict significant and measurable effects due to surface relaxation.[1-3] (2) Although these calculations are based on a shell model which adequately reproduces the bulk dynamics, the results suggest that *surface* phonon dispersion curves, particularly for the heavy alkali halides, are more sensitive to the details of the model. Hence, surface dynamics measurements are needed to validate the use of shell models as a general treatment of the lattice dynamics of ionic crystals.[1-4] (3) The cation and anion masses of RbBr are nearly the same, which leads to predicted dynamical features that arise from "extended" symmetry.[5,6]

Several theoretical calculations have now been carried out for the surface dynamics of alkali halide crystals.[1-3,7] They are all based on a shell-model description, with the parameters obtained by fitting the phonon dispersion curves of the bulk crystal. (The calculations for RbBr are based on an 11-parameter model.) Recently, a new procedure has been employed to allow for the relaxation of the surface within the context of the shell model. For the lighter alkali halides very little difference is found between the relaxed and unrelaxed surface calculations. However, for RbBr the differences are quite remarkable,[1-3] the principal one being the emergence of a surface-localized optical mode lying *above* the optical band structure.[2] This is a sagittally polarized mode and should have a favorable probability for being detected by inelastic He-atom-scattering experiments. In addition to this feature, there are more subtle effects on the energies and widths of all the surface-localized modes, particularly for the optical modes. All of these predictions then offer the opportunity to provide a comparison between experiment and theory and, especially, an evaluation of the ability of the shell model to interpret correctly the surface dynamical behavior.

Foldy and co-workers have recently developed the concept of "extended symmetry" for alkali halides when the anion and cation masses are nearly the same.[5,6] The simplest approximation (or the "textbook example"[8]) of a linear alkali halide "chain" considers only the interactions between nearest neighbors. When the masses of the atoms become equal, the diatomic chain becomes equivalent to a monatomic chain with a lattice spacing half the actual lattice spacing and an apparent Brillouin zone twice as large as the true one. Further, for the monatomic chain there only exists an acoustic branch of the dispersion curve. Thus, the optical branch in the true Brillouin zone can be thought of as that part of the quasimonatomic acoustic branch which extends from the true zone edge to the apparent zone edge, "folded back" into the true zone. In this limiting behavior, one would expect the acoustic and optical branches to meet at the true zone boundary.

Since the vibrations in the high-symmetry directions of cubic crystals behave analogously, one can expect a similar situation in certain directions of real crystals. Thus, Foldy *et al.* have pointed out that the folding for "isobaric" fcc crystals such as NaF, KCl, and RbBr should occur about the hexagonal face of the fcc Brillouin zone, and, in particular, at the points L and W and the straight line Q joining them.[5,6] They cite substantial experimental

and modeling evidence to justify their position.

In studies of the surface dynamics of alkali halides to date, three examples have arisen where a mode has been observed to cross obliquely the acoustic band from very near the band edge at the $\bar{M}$ or $\bar{X}$ point towards the zone center. The first case of a "crossing mode" was in a limited examination of the KCl(001) surface, in the $\langle 100 \rangle$ direction, where a few points of what appears to be an optical branch were observed to "meet" the Rayleigh branch, S_1, at the zone edge.[9,10] In a later, more extensive work Benedek and co-workers extended the ideas of Foldy and co-workers to the surface dynamics of the isobaric alkali halides and compared their predictions to experimental surface dispersion curves for NaF ($m_{Na}=23$ amu, $m_F=19$ amu).[11] Their argument is that the L point at the center of the hexagonal, fcc folding plane in the three-dimensional Brillouin zone becomes the $\bar{X}$ point in the fcc (001) surface Brillouin zone. Folding in the two-dimensional Brillouin zone then takes place with respect to a "folding line" which connects the $\bar{X}$ and the $\bar{M}$ points. (The latter point lies at the two-dimensional zone edge in the $\langle 100 \rangle$ direction.) Benedek and co-workers emphasize the "folded" nature of the possible crossing modes in the $\langle 110 \rangle$ direction and suggest that, at the surface Brillouin-zone boundary, S_8 is the folded optical branch associated with the S_1 Rayleigh modes and that the quasilongitudinal branch S_4 is the folded portion for the acoustic longitudinal S_6 modes. They, however, did not address directly what the effect of folding would be in the $\langle 100 \rangle$ direction. However, if one studies the curves shown in Fig. 1 of Ref. 11, it is clear that the isobaric case must also have a folded branch in the $\langle 100 \rangle$ direction and this is likely the crossing mode observed in KCl.

The third discussion of crossing modes was given by de Wette and co-workers[12] in a detailed theoretical examination of NaCl. They refer to the crossing mode that appears in their calculations as a "sagittal resonance" which arises from the hybridization of acoustic and optical modes. Since NaCl is really not an isobaric alkali halide ($m_{Na}=23$ amu, $m_{Cl}=35.5$ amu), it appears that this behavior results from a different mechanism than that in KCl and NaF.

It seems that there are two mechanisms for crossing modes: a geometric folding, as described by Benedek *et al.*,[7,10] which occurs for equal-mass crystals, and the sagittal resonance, which can occur even when the masses are quite different. In experiments carried out in this laboratory on KBr, we observed a crossing resonance which would appear to be an example of the latter type.[13] In this paper, because the masses of the Rb^+ and Br^- are nearly the same, geometric folding is believed to be the correct description of the crossing resonance. Hence, we will use the term "folding mode" in what follows.

We have embarked on an extensive experimental investigation of the surface dynamics of the alkali halides to understand and to clarify these concepts which we believe will lead to more general models for the entire class of ionic insulators.[13,14] We report, in this paper, the results of inelastically scattered He-atom experiments on the nearly isobaric crystal RbBr in ($m_{Rb}=85.5$ amu, $m_{Br}=79.9$ amu). In Sec. II we describe briefly our time-of-flight scattering instrument. We follow with experimental results and a comparison to the calculations in Sec. III and a discussion of the results in Sec. IV.

II. EXPERIMENT

The He-atom-scattering apparatus for measuring the angular distributions and time-of-flight (TOF) spectra from the RbBr(001) crystal surface has been described previously.[13] Briefly the instrument is an ultrahigh-vacuum (UHV) system consisting of several chambers connected together. It is of the fixed geometry type with a 90° beam source-crystal–detector angle. That is, to be detected, the He-atom incident and scattering angles, θ_i and θ_f, respectively, both measured with respect to the normal of the crystal surface, must satisfy $\theta_i+\theta_f=90°$. The He-beam source is a 30-μm-diam, high-pressure nozzle which produces a nearly monoenergic He beam ($\Delta E/E \approx 2\%$).[15] In these experiments the He pressure and nozzle temperature were chosen so that the incident He wave vector $k_i \approx 7$ Å^{-1} and the beam energy $E_i=\hbar^2 k_i^2/2m \approx 25$ meV.

The crystal is mounted on a manipulator which allows it to be oriented in the proper scattering plane, and heated and cooled over the range of 110–1200 K. The incident angle θ_i—and hence also θ_f—in these experiments can be varied by rotating the crystal on the manipulator with a stepper motor. Because of the relatively low surface Debye temperature of the RbBr crystal (~ 100 K), in all the experiments reported here the crystal was cooled to $T_s \approx 115$ K. The flight path from the crystal to the detector entrance is 1060 mm. The He-atom detector is a quadrupole mass spectrometer with a Channeltron electron multiplier operated in the pulse-counting mode. The data collection is automated under computer control.

The RbBr crystal is of NaCl structure (fcc), has a lattice spacing of 6.85 Å, and is nearly isobaric in the masses of the Rb and Br.[16,17] For these experiments a target sample was prepared by cleaving a RbBr boule in air and then quickly transferring a piece of the proper size (nearly rectangular 5–8 mm on a side and ~ 2 mm thick) onto the manipulator. The scattering chamber was then immediately evacuated. After baking out the chamber at 150 °C for approximately 24 h, the target was flashed to ~ 500 °C. At this point the crystal surface was aligned with respect to the instrument scattering geometry and the measurements could be started. To avoid any problems with physisorption at the low surface temperatures employed, the target was periodically flashed (about every 20 h). The illuminated surface area on the target is estimated to be about 5 mm.^{2} Measurements were taken in the two high symmetry directions, $\langle 100 \rangle$ and $\langle 110 \rangle$, on the natural (001) cleavage plane.

III. RESULTS

A. Angular distributions

Figures 1–3 show angular distributions of scattered He-beam intensity against incident angle θ_i for the two

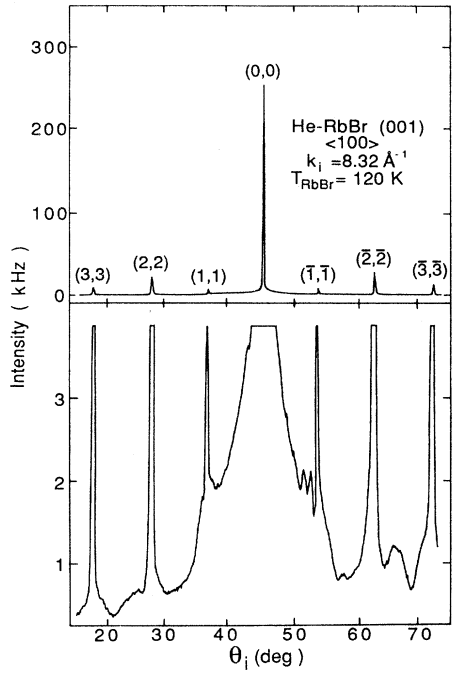

FIG. 1. Intensity of scattered He vs incident angle from RbBr(001) surface in the ⟨100⟩ direction with He-atom wave vector $k_i = 8.32$ Å^{-1}. The lower panel has had the vertical scale expanded by a factor of 100. The intensities are given in kHz.

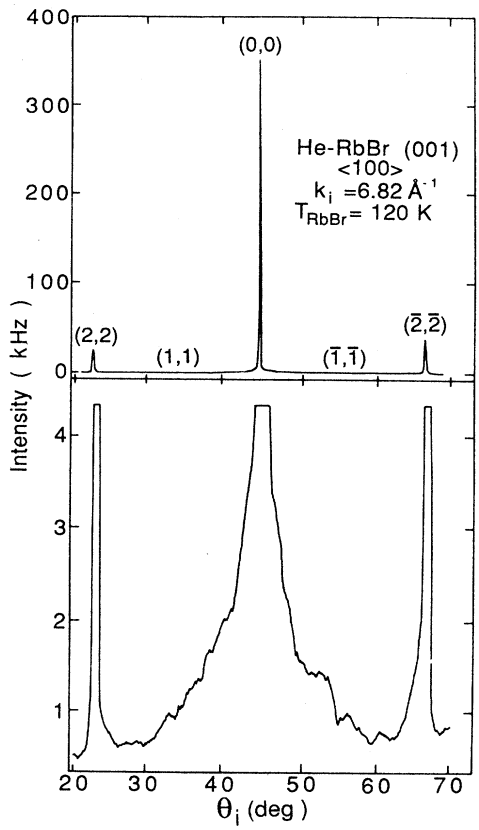

FIG. 2. Intensity of scattered He vs incident angle from RbBr(001) surface in the ⟨100⟩ direction with He-atom wave vector $k_i = 6.82$ Å^{-1}. The lower panel has had the vertical scale expanded by a factor of 100. At this wave vector the first Bragg peaks are missing. The intensities are given in kHz.

high-symmetry directions. The upper panels show the full angular distributions, while the lower ones have the ordinate scale expanded by a factor of 100. The specular and diffraction peaks are narrow in angular spread [for the specular, the full width of half maximum (FWHM) is $\approx 0.1°$], in agreement with that expected ($\sim 0.15°$). The positions of the peaks confirm the lattice spacing of the crystal given above, in agreement with that obtained by other means.[17] The structure in the angular distributions seen in the lower curves of these figures, particularly around the base of the Bragg and specular peaks, is attributed to the inelastic-scattering events, some of which are due to bound-state resonances.[18–20] Figure 2 is rather interesting, for at that wave vector, $k_i = 6.82$ Å^{-1}, the (1,1) and the $(\bar{1},\bar{1})$ Bragg peaks are missing because of interference effects. In terms of the simple eikonal approximation, which has been used to describe the elastic-scattering intensities, this absence corresponds to a zero in the J_1 Bessel function.[21] From this, one can estimate the peak-to-peak corrugation of RbBr to be about 0.4 Å, which is nearly the same as for KBr.[13] We defer a discussion of the energies of the bound states in the He-RbBr potential to a later paper.

B. TOF spectra

Figures 4 and 5 display representative series of TOF spectra for the ⟨100⟩ and ⟨110⟩ directions, respectively, in order to illustrate the quality of the data. The general shape of the spectra is of a broad "hump" with sharp peaks sticking out. The hump is due to the inelastic He scattering from bulk-phonons, which on the surface are spread in energy into broad bands, and also to multiphonon scattering.[22]

The sharp peaks arise from single-He-phonon scattering events. From the arrival-time spectrum at a particular incident angle, θ_i, one can calculate the He momentum transfer parallel to the surface, $\Delta\mathbf{K}$, and the energy transfer, $\hbar\omega$.[10] The first of these is related to the phonon wave vector by

$$\Delta\mathbf{K} \equiv \mathbf{K}_f - \mathbf{K}_i = \mathbf{G} + \mathbf{Q} , \tag{1}$$

where $\mathbf{K}_f$ and $\mathbf{K}_i$ are the surface projections of the final and incident wave vectors $\mathbf{k}_f$ and $\mathbf{k}_i$, respectively, $\mathbf{G}$ is the surface reciprocal-lattice vector for the crystal, and $\mathbf{Q}$ is the surface projection of the phonon wave vector. The phonon energy is just the final He energy minus the initial He energy, or

$$\hbar\omega = \hbar^2(k_f^2 - k_i^2)/2m , \tag{2}$$

where a positive value for ω means that a phonon has been annihilated and a negative value means that a phonon has been created in a single-collision event. The in-

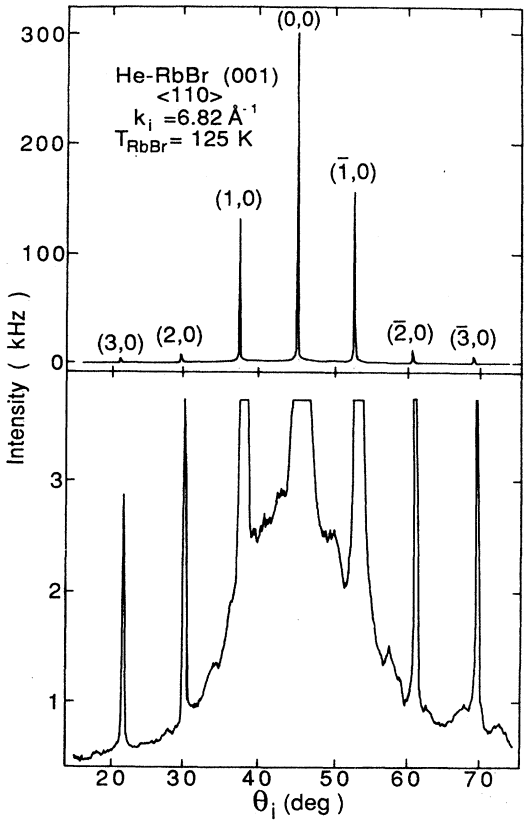

FIG. 3. Intensity of scattered He vs incident angle from RbBr(001) surface in the ⟨110⟩ direction with He-atom wave vector $k_i = 6.82$ Å^{-1}. The lower panel has had the vertical scale expanded by a factor of 100. The intensities are given in kHz.

terpretation of the peaks of several of the spectra of Fig. 4 in terms of phonon energy and wave vector are shown in Fig. 6. The heavy dark curves are the calculated dispersion curves adapted from Ref. 3, while the lighter lines are called scan curves[10] and represent the combination of Eqs. (1) and (2),

$$\hbar\omega/E_i = [(\Delta K + k_i \sin\theta_i)^2/k_i^2\cos^2\theta_i] - 1 \ . \quad (3)$$

Because the scan curves contain the kinematic requirements for the creation or annihilation of single phonons by the He atoms, a peak occurs in the TOF where the scan curve and dispersion curve cross. (Occasionally, a peak will also occur for a bulk phonon with a high surface density of states.) In the examples shown in Fig. 6, one can see that the points are usually close to the calculations of de Wette and co-workers, but not exactly. Since Eq. (3) contains neither any dynamical information, such as cross sections, nor experimental signal-to-noise requirements not every crossing point will necessarily show up in the TOF spectra.

C. Dispersion curves

The results of approximately 60 TOF spectra are presented in Fig. 7. In panel (a) the data are compared with the slab calculation of the surface dynamics which does *not* take into account any surface relaxation.[3] In panel (b) the same data are compared with a similar calculation, based on the same shell model, but where the surface has been allowed to relax.[1–3] The Rayleigh mode and the associated folded mode are clearly in evidence, as expected of the isobaric crystal, along with several points representing the S_6 longitudinal-acoustic surface reso-

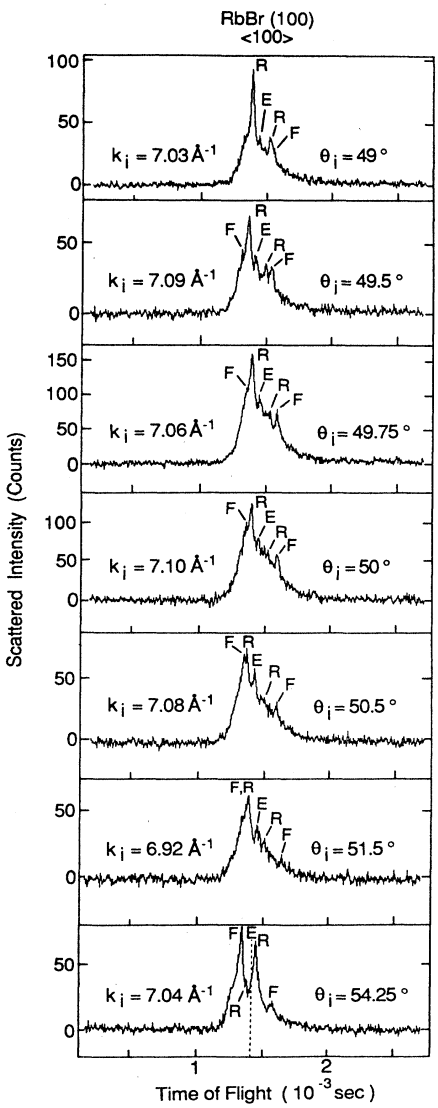

FIG. 4. Representative series of time-of-flight spectra of inelastically scattered He from RbBr(001) in the ⟨100⟩ direction for $k_i \simeq 7$ Å^{-1} at several incident angles. The letter E or the dashed line marks the diffuse elastic-peak position or arrival time, while R and F refer to the Rayleigh and folded modes, respectively. The peaks at times longer than the elastic position arise from creation events, while the peaks at shorter times are from annihilation events. Each point on the histogram corresponds to 6 μs.

nance in the $\bar{\Gamma}\bar{X}$ region of the surface Brillouin zone. There are, in addition, some data points with relatively weaker intensities which lie near the longitudinal-acoustic resonance in the $\bar{\Gamma}\bar{M}$ region and near the longitudinal-optical band edge in the $\bar{\Gamma}\bar{X}$ region. However, there are *no* points that are observed to be near the S_2 mode, which is predicted to lie above the optical bands in the relaxed RbBr surface.

IV. DISCUSSION

In comparing the agreement between the experiments and the slab calculations in Fig. 7, it seems natural to start from the bottom and work upwards. (i) The calculations and the measurements for the Rayleigh modes appear to agree quite well in both panel (a) and (b). (ii) There also seems to be reasonably good agreement in both with the longitudinal-acoustic resonance. However, because there is not much data along this resonance, and most of the more intense TOF peaks were measured in the ⟨110⟩ direction, it is difficult to draw any firm conclusions from these results. (iii) With the folded modes, however, there is some difference in the fits in two respects. First, the calculation that includes the surface relaxation predicts a broad resonance [broad hatched regions in Fig. 7(b) as opposed to the sharp surface-localized mode shown by a line in Fig. 7(a)], which implies that the corresponding TOF peaks should also be rather broad.[2] This is not what is observed experimentally. The TOF peak shapes for the folded modes are as sharp as those for the Rayleigh modes, in agreement with the calculation for the unrelaxed surface. Second, the measured phonon energies are much closer to the calculated valued in panel (a) than in (b). (iv) Of importance is the *absence* of data that match the high-lying S_2 branch in Fig. 7(b). Normally, there is a great reluctance to draw any conclusion from a negative result. However, in the investigation in this laboratory of the surface dynamics of the KBr crystal,[13] the S_2 branch that is predicted to lie in the gap between the acoustic and optical bands with about the same phonon energies as predicted for the S_2 modes of RbBr was clearly found. In fact, the intensity of the S_2 peaks in many of the TOF spectra for KBr were comparable to those of the Rayleigh modes. Thus, we believe that if this branch existed where it is predicted in Fig. 7(b) and had a comparable cross section to the analogous mode in KBr, we would have seen it.

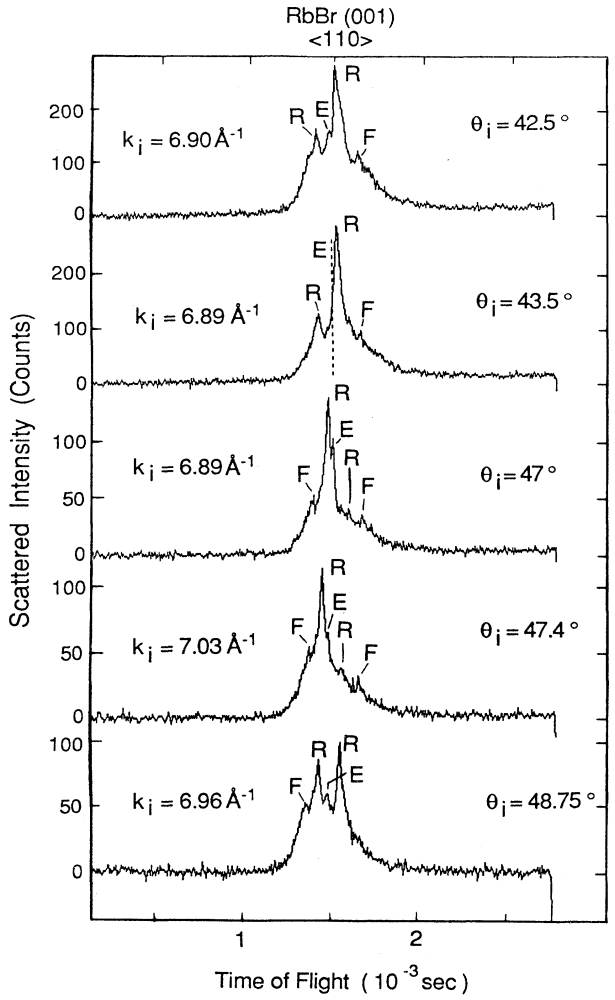

FIG. 5. Representative series of time-of-flight spectra of inelastically scattered He from RbBr(001) in the ⟨110⟩ direction for $k_i \simeq 7$ Å^{-1} at several incident angles. The designations of the peaks are as described in Fig. 4.

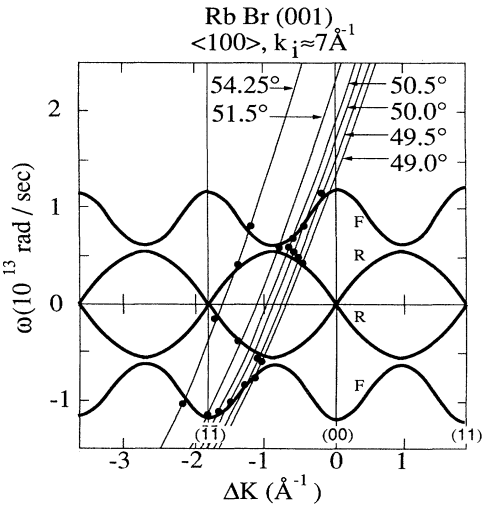

FIG. 6. The heavy dark curves are the Rayleigh and folded dispersion modes adapted from the unrelaxed slab calculations (Ref. 3) for RbBr(001) in $\bar{\Gamma}\bar{M}$, plotted in an extended representation as phonon frequency vs ΔK. Several scan curves (thin lines) calculated from Eq. (3) with wave vector and incident angles of some of the spectra shown in Fig. 4 are also superimposed. The solid points mark the energy and wave-vector position of the peaks labeled in the spectra.

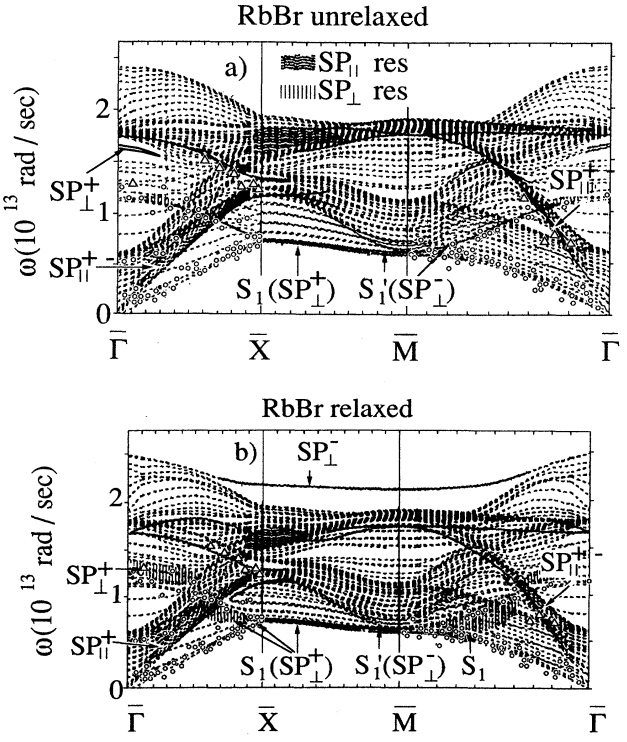

FIG. 7. Dispersion relations for the surface waves of the RbBr(001) surface over the two high-symmetry directions of the surface Brillouin zone. In (a) the calculations are for the unrelaxed surface (Ref. 3), while in (b) the calculations are for a relaxed surface (Refs. 2 and 3). The data are the same in both (a) and (b). The measured values are indicated by open circles, except for those points with relatively weaker intensities, shown by open triangles. The experimental uncertainty in energy is estimated to be ± one circle diameter from the center of each data point.

From the above summary of the results, it is clear that the calculation which does not allow for surface relaxation gives a somewhat better representation of the surface dynamics of RbBr. It is not perfect, by any means, and there are some weak but distinct points which do not seem to lie near any surface-localized resonances. One series of these points appears to come off the longitudinal-acoustic resonance in $\bar{\Gamma}\bar{X}$ near the band edge; the points lie very near the shear horizontal surface mode shown by a solid line in both Figs. 7(a) and 7(b). Since the He-atom probe does not couple to shear horizontal modes, it is suggestive that these points represent the folded portion of the longitudinal-acoustic mode as discussed by Benedek *et al.*[11] If this turns out to be the case, the shell model would need to be modified to bring out this feature. It is also possible that these points are connected with the "missing" S_2 modes that were predicted in the relaxed case to lie above the optical band.[23] A certain amount of caution is appropriate here, of course, because of the low intensity of the corresponding TOF peaks.

Finally, we note that the splittings or energy gap at the $\bar{X}$ and $\bar{M}$ points of the Rayleigh and folded modes appear to be very small. Since the deviations from the quasi-monoatomic rigid-ion model can arise from non-nearest-neighbor interactions, polarizability differences, three-body interactions, etc., as well as from slight mass differences, to give a gap at the zone edge, these effects appear to be small (or compensating) on the surface, just as in bulk RbBr at the L point.[4,5]

Since one's intuition about the nature of the unbalanced forces at the surface suggests that the surface ought to relax, one is left with the conclusion that modifications are needed in the shell-model treatment of the relaxation. Because of the importance of this point, we plan to investigate the surface dynamics of the RbI crystal where the same theoretical treatment also predicts a high-lying S_2 branch. de Wette and co-workers have pointed out that the surface dynamics should be a more stringent test of the shell model and that some of the parameters used for the fit to the bulk RbBr dispersion curves are somewhat unphysical.[1-3] Our results also agree with these authors' expectations that the higher-lying optical modes should be more sensitive to the features of the shell model than the lower-energy acoustic modes.

ACKNOWLEDGMENTS

We acknowledge support from the U.S. Department of Energy under Grant No. DE-FG05-85ER45208. We also want to acknowledge fruitful discussions with Professor F. W. de Wette at the University of Texas at Austin and with Professor J. R. Manson at Clemson University, Clemson, South Carolina.

[1]F. W. de Wette, W. Kress, and U. Schroeder, Phys. Rev. B **32**, 4143 (1985).
[2]W. Kress, F. W. de Wette, A. D. Kulkarni, and U. Schroeder, Phys. Rev. B **35**, 5783 (1987).
[3]F. W. de Wette, A. D. Kulkarni, U. Schroeder, and W. Kress, Phys. Rev. B **35**, 2476 (1987).
[4]H. Bilz and W. Kress, in *Phonon Dispersion Relations in Insulators* (Springer, New York, 1979).
[5]L. L. Foldy and T. A. Whitten, Jr., Solid State Commun. **37**, 709 (1981).
[6]B. Segall and L. L. Foldy, Solid State Commun. **47**, 593 (1983).
[7]G. Benedek and L. Miglio, in *Ab Initio Calculations of Phonon Spectra,* edited by J. Devreese, V. E. van Doren, and P. E. van Camp (Plenum, New York, 1982).
[8]C. Kittel, *Introduction to Solid State Physics* (Wiley, New York, 1986).
[9]G. Benedek, G. Brusdeylins, R. B. Doak, and J. P. Toennies, J. Phys. (Paris) Colloq. Suppl. 12 **42**, C6-793 (1981).
[10]G. Brusdeylins, R. B. Doak, and J. P. Toennies, Phys. Rev. B **27**, 3662 (1983).
[11]G. Benedek, L. Miglio, G. Brusdeylins, J. G. Skofronick, and J. P. Toennies, Phys. Rev. B **35**, 6593 (1987).
[12]F. W. de Wette, W. Kress, and U. Schroeder, Phys. Rev. B **33**, 2835 (1986).

[13]G. Chern, J. G. Skofronick, W. P. Brug, and S. A. Safron, this issue, Phys. Rev. B **39**, 12 828 (1989).
[14]G. Chern, W. P. Brug, S. A. Safron, and J. G. Skofronick, J. Vac. Sci. Technol. (to be published).
[15]J. P. Toennies and K. Winkelmann, J. Chem. Phys. **66**, 3965 (1977).
[16]Crystal Growth Laboratory, Department of Physics, University of Utah, Salt Lake City, UT 84112.
[17]R. W. G. Wyckoff, *Crystal Structures* (Wiley, New York 1964), Vol. 1.
[18]G. Boato and P. Cantini, Adv. Electron. Electron Phys. **60**, 95 (1983).
[19]D. Evans, V. Celli, G. Benedek, J. P. Toennies, and R. B. Doak, Phys. Rev. Lett. **50**, 1854 (1983).
[20]D. Eichenauer and J. P. Toennies, J. Chem. Phys. **85**, 532 (1986).
[21]U. Garibaldi, A. C. Levi, R. Spadacini, and G. E. Tommei, Surf. Sci. **48**, 649 (1975).
[22]J. P. Toennies, *Proceedings of the Solvay Conference on Surface Science, Austin, 1987,* in *Springer Series in Surface Science* (Springer, New York, in press).
[23]F. W. de Wette (private communication).